PCCP

CORRECTION

View Article Online
View Journal | View Issue

Cite this: *Phys. Chem. Chem. Phys.*, 2018, **20**, 24490

DOI: 10.1039/c8cp91852j

rsc.li/pccp

Correction: Two-dimensional nitrides as highly efficient potential candidates for CO_2 capture and activation

Raul Morales-Salvador, Ángel Morales-García, Francesc Viñes and Francesc Illas*

Correction for 'Two-dimensional nitrides as highly efficient potential candidates for CO_2 capture and activation' by Raul Morales-Salvador *et al.*, *Phys. Chem. Chem. Phys.*, 2018, **20**, 17117–17124.

The authors would like to correct errors associated with the reported PBE calculations. Due to a problem in the backup of some of the output files, the reported PBE results for the clean surfaces do not correspond to the fully relaxed structure. Once the proper energies are used, the E_{ads} (PBE) values become on average 0.34 eV larger thus favoring adsorption. This implies that E_{ads} (PBE-D3) values are larger than PBE ones by 0.30 eV and not 0.7–1.0 eV as reported in *Phys. Chem. Chem. Phys.*, 2018, **20**, 17117–17124. As a consequence, desorption temperatures predicted by the PBE calculations need to be corrected becoming higher.

The error found in the set of PBE results does not affect the main conclusion of the manuscript based on the more accurate PBE-D3 method indicating that 2D nitrides are potential materials for the capture and activation of CO_2. Updated versions of Fig. 2 and Tables S1 and S3 are included.

Departament de Ciència de Materials i Química Física & Institut de Química Teòrica i Computacional (IQTCUB), Universitat de Barcelona, c/ Martí i Franquès 1, 08028 Barcelona, Spain. E-mail: francesc.illas@ub.edu; Fax: +34-93-402-1231; Tel: +34-93-402-1229

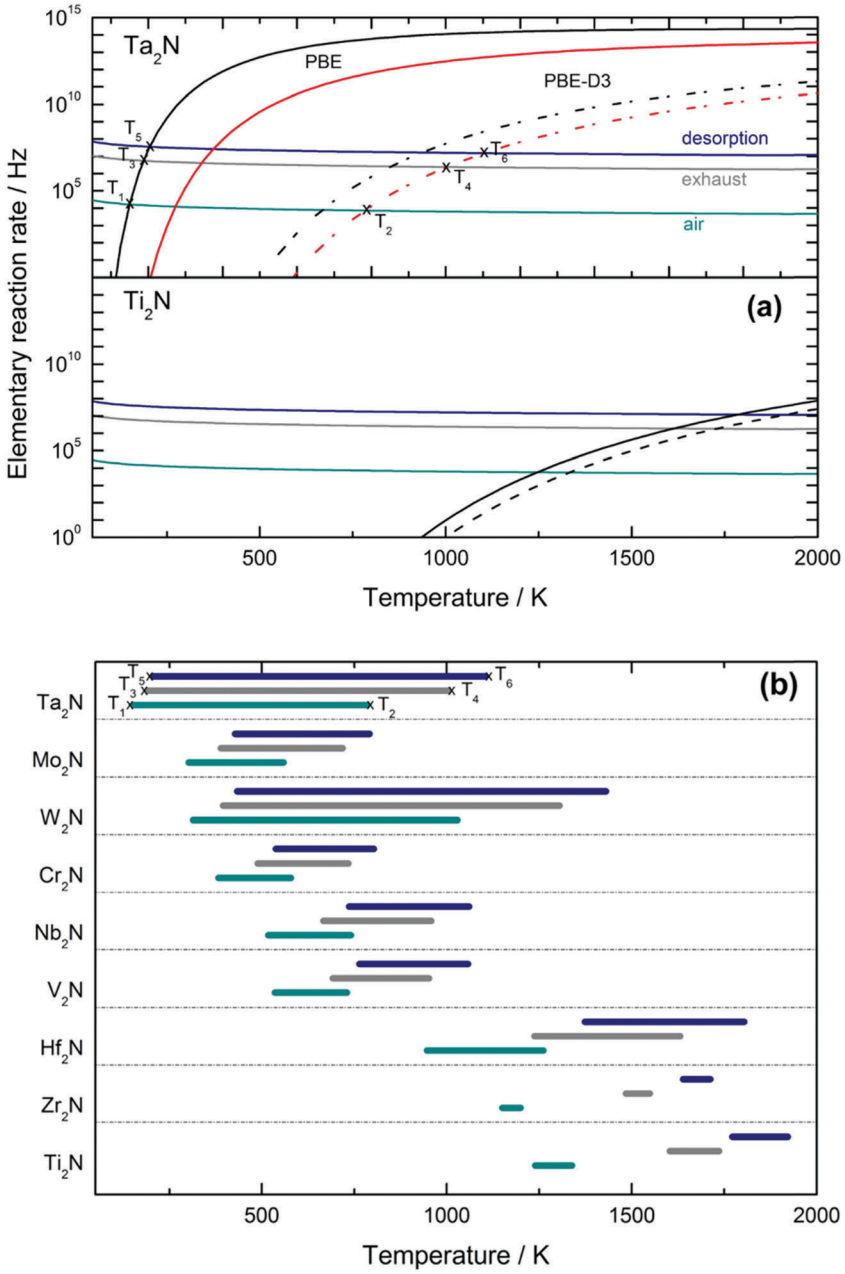

Fig. 2 (a) Calculated rates for desorption and adsorption of CO_2 on Ta_2N and $Ti_2N(0001)$ surfaces. On Ta_2N marked points with T_1–T_6 labels show how desorption temperature ranges, in (b), have been obtained. In (a), green, gray and blue colors correspond to adsorption rates on a single site per time unit for a CO_2 partial pressure of 40, 15×10^3, and 10^5 Pa, respectively. Black and red lines are desorption rates per site for E_{ads} obtained from PBE (solid) and PBE-D3 (dashed) calculations. In (b), green, gray, and blue bars belong to desorption temperature ranges for CO_2 partial pressures of 40, 15×10^3, and 10^5 Pa, respectively.

Table S1 Adsorption energy (in eV) of CO_2 molecule on MXene carbides at PBE and PBE-D3 levels on the adsorption sites described in Fig 1. Bond lengths δ(CO) and δ(MO) are given in Å, as well as the CO_2 molecular angle, α(OCO), in degrees. The Bader charge analysis, ΔQ, is given in e and corresponds to charge difference between the adsorbed and isolated CO_2 molecule

MXene	Level	E_{ads}[a]	δ(MO)	δ(CO)	α(OCO)	ΔQ
			η^1-CO_2-μ^2-C_B			
Cr_2N	PBE	−0.98	2.10 (×2)	1.26 (×2)	136.8	−0.89
	PBE-D3	−1.30	2.10 (×2)	1.26 (×2)	136.8	−0.90
Hf_2N	PBE	−2.16	2.18 (×2)	1.29 (×2)	130.1	−1.47
	PBE-D3	−2.29	2.18 (×2)	1.29 (×2)	129.9	−1.47
Nb_2N	PBE	−1.42	2.24 (×2)	1.27 (×2)	132.6	−1.11
	PBE-D3	−1.73	2.23 (×2)	1.27 (×2)	132.4	−1.12
Ta_2N	PBE	−1.62	2.16 (×2)	1.28 (×2)	132.4	−1.20
	PBE-D3	−1.90	2.16 (×2)	1.28 (×2)	132.4	−1.21
V_2N	PBE	−1.39	2.11 (×2)	1.27 (×2)	134.6	−1.08
	PBE-D3	−1.67	2.10 (×2)	1.27 (×2)	134.6	−1.08
Mo_2N	PBE	−0.98	2.24 (×2)	1.26 (×2)	136.2	−1.06
	PBE-D3	−1.33	2.23 (×2)	1.26 (×2)	136.2	−1.06
W_2N	PBE	−0.76	2.22 (×2)	1.26 (×2)	136.8	−0.86
	PBE-D3	−1.21	2.22 (×2)	1.26 (×2)	136.7	−0.86
			η^2-CO_2-μ^3-C_MO_B			
Nb_2N	PBE	−1.38	2.40;2.39	1.26;1.33	130.8	−1.35
	PBE-D3	−1.69	2.39 (×2)	1.26;1.33	130.9	−1.35
V_2N	PBE	−1.36	2.25;2.24	1.26;1.32	133.1	−1.30
	PBE-D3	−1.65	2.23;2.25	1.26;1.32	133.1	−1.30
Mo_2N	PBE	−0.68	2.36;2.36	1.26;1.30	134.7	−1.39
	PBE-D3	−1.03	2.35;.2.36	1.26;1.30	134.7	−1.39
			η^2-CO_2-μ^3-C_NO_B			
Cr_2N	PBE	−0.88	2.22;2.18	1.25;1.31	135.0	−1.12
	PBE-D3	−1.21	2.22;2.17	1.25;1.31	135.0	−1.14
Nb_2N	PBE	−1.18	2.39;2.36	1.26;1.33	132.1	−1.34
	PBE-D3	−1.50	2.39;2.36	1.26;1.33	132.2	−1.35
V_2N	PBE	−1.21	2.26;2.21	1.26;1.32	133.9	−1.32
	PBE-D3	−1.51	2.25;2.21	1.26;1.33	134.0	−1.32
			η^3-CO_2-μ^5-$C_MO_NO_N$			
Zr_2N	PBE	−2.72	2.34;2.352.34;2.35	1.36 (×2)	116.2	−1.79
	PBE-D3	−2.83	2.34;2.352.34;2.35	1.36;1.37	116.2	−1.80
Hf_2N	PBE	−2.82	2.32;2.33	1.35;1.44	114.0	-2.02
	PBE-D3	−2.97	2.22;2.33	1.35;1.44	114.0	−2.02
Ti_2N	PBE	−2.92	2.23 (×2)	1.40;1.36	115.9	−1.86
	PBE-D3	−3.13	2.23;2.192.23;2.16	1.40;1.36	115.9	−1.87
			η^3-CO_2-μ^5-$C_NO_MO_M$			
Ta_2N	PBE	−1.60	2.00 (×2)	1.38 (×2)	112.8	−1.65
	PBE-D3	−1.89	2.00 (×2)	1.38 (×2)	112.8	−1.65
W_2N	PBE	−1.30	2.00 (×2)	1.37 (×2)	114.0	−1.40
	PBE-D3	−1.77	2.00 (×2)	1.37 (×2)	114.0	−1.40
Ti_2N	PBE	−2.92	2.20;2.14(×2)	1.39;1.40	115.3	−1.94
	PBE-D3	−3.13	2.20;2.13(×2)	1.39;1.40	115.2	−1.94
			η^2-CO_2-μ^4-O_BO_B			
Ta_2N	PBE	−0.30	2.10;2.30(×2)	1.39 (×2)	106.8	−1.62
	PBE-D3	−0.61	2.10;2.31(×2)	1.39 (×2)	106.8	−1.63
			η^3-CO_2-μ^4-$C_BO_BO_B$			
Mo_2N	PBE	−0.98	2.22;2.282.19;2.31	1.38;1.36	111.2	−1.81
	PBE-D3	−1.34	2.22;2.282.19;2.31	1.38;1.36	111.2	−1.82
Cr_2N	PBE	−1.08	2.09;1.982.05;2.25	1.39;1.29	121.3	−1.27
	PBE-D3	−1.44	2.08;1.972.05,2.25	1.39;1.29	121.3	−1.28
			η^3-CO_2-μ^4-$C_MO_MO_B$			
W_2N	PBE	−2.20	2.17;2.04	1.33;1.39	116.5	−1.41
	PBE-D3	−2.59	2.17;2.04	1.33;1.39	116.5	−1.41

[a] ZPE corrected as above stated.

Table S3 Desorption temperature range ([PBE]–[PBE-D3]) for CO_2 partial pressure ranges for CO_2 partial pressures of 40, 15×10^3, and 10^5 Pa, which stand for air, exhaust, and desorption situations, respectively. All temperature values are given in K

	Temperature range		
MXene	Air	Exhaust	Desorption
η^1-CO_2-μ^2-C_B			
Cr_2N	415–548	529–704	581–776
Hf_2N	946–1004	1237–1316	1373–1463
Nb_2N	607–741	782–958	864–1060
Ta_2N	669–784	853–1004	937–1104
V_2N	594–715	765–924	844–1023
Mo_2N	412–559	526–718	577–791
W_2N	314–498	395–634	433–696
η^2-CO_2-μ^3-C_MO_B			
Nb_2N	591–726	763–938	842–1037
V_2N	603–730	786–952	871–1057
Mo_2N	302–453	389–586	428–648
η^2-CO_2-μ^3-C_NO_B			
Cr_2N	383–523	489–672	538–741
Nb_2N	517–650	666–843	736–934
V_2N	535-661	692–859	764–949
η^3-CO_2-μ^5-$C_MO_NO_N$			
Zr_2N	1150–1199	1484–1549	1639–1712
Hf_2N	1138–1261	1449–1631	1591–1804
Ti_2N	1239–1338	1603–1735	1772–1921
η^3-CO_2-μ^5-$C_NO_MO_M$			
Ta_2N	646–761	815–962	890–1053
W_2N	512–697	641–877	697–956
Ti_2N	1239–1339	1603–1736	1773–1922
η^2-CO_2-μ^4-O_BO_B			
Ta_2N	152–276	191–344	205–377
η^3-CO_2-μ^4-$C_BO_BO_B$			
Mo_2N	408–531	515–669	563–729
Cr_2N	444–579	560–734	611–803
η^3-CO_2-μ^4-$C_MO_MO_B$			
W_2N	872–1029	1102–1305	1205–1430

The Royal Society of Chemistry apologises for these errors and any consequent inconvenience to authors and readers.